Tel-Aviv University
Faculty of Exact Sciences
Department of Geophysics and Planetary Sciences

Master of Science Thesis

Contribution of grains to the opacity of a protoplanetary atmosphere

by

Naor Movshovitz

Supervisor: Morris Podolak

Tel-Aviv, 2007

Abstract

The opacity of a protoplanetary atmosphere is estimated by determining the size distribution of solid grains in the atmosphere, allowing for sedimentation of grains and for growth by coagulation. The opacity of the radiative envelope is an important parameter for modeling planet formation. Solid grains provide a major contribution to the opacity at lower temperatures, however, the actual value of the grain opacity is difficult to determine. The importance of this parameter, the opacity, lies in the fact that it limits the rate at which energy is radiated away from the planet, thus controlling the cooling rate of the planet. The uncertainty in the value of the opacity stems from the fact that the solid grains present in the protoplanetary atmosphere cannot be assumed to have the same size distribution as grains in interstellar gas. The grains spend enough time in the atmosphere to change their size distribution considerably by collision induced growth. Models of planet formation (Hubickyj et al., 2005) have assumed that this growth leads to a reduction in opacity values to a fraction of those calculated with an interstellar grain size distribution. Here I try to test this assumption by using a computer code to estimate an appropriate size distribution for grains in a protoplanetary atmosphere, and the resulting opacity. For a wide range of model parameters, I find that (1) the grain size distributions reach a steady state in a short time compared with the time scale of planet formations, and (2) these size distributions result in opacity profiles that are high in the upper layers of the atmosphere but drop sharply so that in much of the atmosphere's radiative zone the opacity is as low as previously assumed, or lower. Implications for planet formation models are discussed.

Contents

Chapter 1

Introduction

The planets in our solar system were formed from material left over after the formation of the Sun, but the details of the formation process are still under investigation. It is believed that the giant gaseous planets of our solar system, Jupiter and Saturn, have a solid core embedded in the gaseous atmosphere. The leading theory on the formation of these planets supposes that they were formed in two stages: The solid core was first formed by coagulation of planetesimals in the protoplanetary disk, the disk of leftover material from the formation of the star. Then, when the core became massive enough to gravitationally attract and capture gas from the disk, the gaseous envelope was formed. Detailed calculations and numerical simulations of these formation stages have been performed (Pollack et al., 1996; Hubickyj et al., 2005) and the resulting model is known as the *core accretion–gas capture model*, or as *core nucleated accretion*, or simply as the *core accretion model*.

To successfully explain the formation of planets the core accretion model must account (as does any competing theory) for the observed properties of the giants planets. In particular:

1. As mentioned before there is evidence that the two gas giants possess a solid core embedded in the gaseous envelope. There is some uncertainty as to the size of the solid cores but often quoted numbers are $5-10$ $M_\oplus$ for Jupiter and $10-20$ $M_\oplus$ for Saturn (Saumon and Guillot, 2004). The remainder of the mass is in the form of a gaseous H_2 and He envelope, leaving Jupiter and Saturn with very massive envelopes[1].

2. The atmospheres of the gas giants are enriched with heavy elements compared with the solar abundance. The degree of enhancement varies from a factor of $1.5-6$ for Jupiter to $6-14$ for Saturn (Saumon and Guillot, 2004).

Detailed simulations based on the core accretion model have been carried out (Pollack et al., 1996; Hubickyj et al., 2005), that begin with a small solid nucleus of less than one Earth mass and end with an almost fully formed planet. These simulations show three distinct phases. During the first phase the planet still consists primarily of solid material, the gas accretion rate is small, and the planetesimal accretion rate increases rapidly until the planet's feeding zone is

[1]The total masses are $\sim$318 $M_\oplus$ for Jupiter, $\sim$95 $M_\oplus$ for Saturn.

depleted. The planet then enters a second phase during which the rates of solid and gas accretion are both small and nearly constant. When the gas mass of the planet is about equal to its solid mass the third phase begins, characterized by runaway accretion of gas.

Simulations of this kind, using reasonable parameters, have been successful in producing "planets" with properties similar to those of the actual giant planets, but there are some concerns about the theory that still trouble researchers. One major point of concern is that the formation time for a Jupiter-like planet at 5 AU from a Sun-like star is uncomfortably close to the estimated lifetime of the protoplanetary disk in which it is to be formed. Observations of disks around young stars give estimates of 0.1–10 Myr for the lifetime (Haisch et al., 2001), while numerical simulations are able to produce a planet in times varying from a few to many millions of years, depending on several key parameters (Hubickyj et al., 2005).

One of these key parameters is the value that numerical models use for the opacity of the gaseous envelope during the second of the phases described above. In particular, the contribution to the opacity from aerosols, small grains of solid material suspended in the gas, is an important factor whose value is uncertain. The importance of this parameter, the opacity of the atmosphere, lies in the fact that it limits the rate at which energy is radiated away from the planet, and thus it is this parameter that controls the cooling rate and contraction of the planet during the second (and far the longest) phase of formation.

Energy is constantly being input into the atmosphere of the young planet. Two major sources of energy are the gravitational energy released by the accretion of gas from the planetary disk and its ensuing contraction, and the constant stream of planetesimals that are captured by the forming planet. This energy is converted into heat energy — it is heating up the planet's atmosphere. This of course causes an increase in the atmospheric pressure, and acts to counter the gravitational force that is compressing the atmosphere to its present density. This energy must be dissipated if the large and diffuse cloud of gas is to become a compact and dense planet.

The dissipation of energy from the planet's surface into space is through radiation. The transfer of energy from the planet's interior to it's surface is achieved through radiation and convection, where one of these processes is usually dominant in some parts of the atmosphere and the other is dominant in other parts. The upper layer of the atmosphere is a "radiative zone", i.e., radiative transfer is the dominant process of energy transfer through this zone, and into space.

The efficiency of energy transfer by radiation depends on how opaque the atmosphere is to photons. This property, the opacity, depends on the temperature and composition of the atmosphere. Furthermore, the opacity is different for different wavelengths of radiation. The composition of the gas in the protoplanet's atmosphere is known – it is the same as the composition of the surrounding disk from which the planet gets its material. But the atmosphere also contains grains of solid material, and these grains too scatter photons and contribute to the opacity of the atmosphere.

The composition of the solid grains is the same as of those grains that are contained in the surrounding disk, and it varies according to the planet's distance from the star – further from the system's heat source the gas temperature

is lower and more substances can condense and exist in the solid phase. But the size distribution of these grains is a different question. Models of planet formation typically use properties of interstellar grains (Pollack et al., 1996), including an interstellar size distribution, for lack of a better option, but the properties of grains that have spent several thousand years in the atmosphere of a protoplanet may be very different from those found in the surrounding disk. Coagulation, fragmentation, and evaporation are all processes that can change the distribution of grain sizes in the planet's atmosphere in the time scale of the planet's formation. A more realistic size distribution of solid grains in the atmosphere is necessary for a calculation of the atmosphere's opacity, particularly when this distribution contains grains that are smaller than, comparable to, and much larger than the wavelengths of strong radiation.

It has been demonstrated (Hubickyj et al., 2005) that an arbitrary lowering of the opacity parameter in the core accretion model can lead to a reduced formation time, a desirable result. The justification for lowering the opacity was that coagulation of small grains into larger ones will lead to faster settling of these grains deeper into the atmosphere where they will be destroyed by the higher temperatures. But it is difficult to estimate, based on qualitative arguments alone, what would be an appropriate value for the grains' contribution to opacity. It is not even clear a priori that coagulation of grains should immediately *reduce* the opacity, for while distributing the same mass of solid matter into larger grains does reduce the surface area that they take up, the larger grains are also, under some circumstances, more efficient scatterers of radiation. While the grains grow and sediment to lower regions, a constant influx of gas brings with it more grains of interstellar size, and planetesimals that enter the planet's atmosphere break up and inject more grains deeper in the atmosphere. All these processes should ideally be accounted for when estimating the total opacity of the atmosphere during the formation period.

Podolak (2003) calculated a grain size distribution in a protoplanetary atmosphere using a grain microphysics code. He used this distribution to estimate the opacity, and found it to be much lower than the interstellar value. The purpose of this work is to make this conclusion more robust by repeating the calculation with greater accuracy, and by exploring further the parameter space. I attempt to identify under what circumstances it is correct to assume that the grain opacity in the context of the core accretion model is much lower than the interstellar value, and to suggest the value that should be used instead.

For this I needed to make a detailed calculation of the size distribution of solid grains throughout the radiative zone of a model protoplanet, and to use this distribution to calculate the grains' contribution to the opacity of the atmosphere. As the equation that describes the coagulation process is not amenable to analytic solution (except in the simplest cases) this had to be done via a computer program that tracks the evolution of the number densities of grains of many sizes as they collide, grow, and sediment through the atmosphere. This kind of program can potentially be computationally demanding and also suffer from numerical errors and so a number of concessions had to be made in the interest of simplicity. In the next chapter I explain the physical processes and equations that are simulated in this program, and justify neglecting those that are not treated. In chapter 3 I describe the program itself and discuss some numerical subtleties. In the last chapter I describe the cases that I ran this program on and the resulting distributions and opacities, and argue that these

results show that the low opacity values used by Hubickyj et al. (2005) are a safe estimate in most cases, and in some cases even lower values can be used. I also suggest ways in which these calculations should be improved to give more accurate results.

Chapter 2

Physical processes

To correctly estimate the grain opacity the size distribution of grains needs to be known at every point in the atmosphere. Solid grains are accreted along with the gas from the solar nebula onto the top of the planet's atmosphere, and solid grains are also deposited deeper in the atmosphere where captured planetesimals ablate and break up due to stress forces. Whatever their source, solid grains in the planet's atmosphere will experience the following processes that act to change their size and location:

1. Solid grains fall through the gas toward the center of the planet. The planet's atmosphere is considered to be in hydrostatic equilibrium and the grains' velocity relative to the gas is assumed to be their true velocity. I will refer to this process, the ordered motion of grains relative to the gas in the radial direction, as *sedimentation*.

2. The grains also have a random component of velocity relative to the gas – their Brownian motion. Also, larger grains sediment faster than smaller grains. Thus there is a relative velocity between all grains. When two grains come into contact as a result of this relative velocity they may stick together to form a larger grain. I will refer to this process as *coagulation*. (*Coalescence* is also often used as well as *collection*, sometimes with subtle differences in meaning, but I will only use coagulation.) When a collision occurs between two grains the result may also be breakup of one or both grains to produce a larger number of smaller grains. Alternatively, the colliding grains may bounce off of each other with no change to their size and mass. Whether grains adhere on collision or break up, or neither, is mainly a question of the collision velocity (see, e.g. Chokshi et al., 1993; Tielens et al., 1994).

3. Solid grains can lose mass through evaporation. The rate of evaporation depends strongly on the composition of the grain and on the ambient temperature. If the partial pressure in the gas phase of the grain species is non-negligible it also effects evaporation rate. If the partial pressure is high enough a grain may also gain mass from the gas phase through recondensation.

Finally, when the size distribution is known, the grains' contribution to opacity should be calculated with a suitable averaging over wavelengths, and

Table 2.1: Typical values of some properties of a model atmosphere.

Property	Value		
Radius (m)	5×10^8	–	5×10^9
Temperature (K)	150	–	650
Density (kg/m^3)	10^{-8}	–	10^{-3}
Acceleration of gravity[a] (m/s^2)	10^{-4}	–	10^{-2}
Viscosity (kg m^{-1} s^{-1})	10^{-5}	–	2×10^{-5}
Mean free path[b] (m)	10^{-5}	–	10^{-1}

[a] With a core of $\sim$10 $M_\oplus$ and total envelope mass of $\sim$2 $M_\oplus$

[b] With a mean molecular weight of 2.3 g/mol and a collision cross-section of 10^{-15} cm^2 for the atmospheric gas.

accounting for the varying (with wavelength) real and imaginary refractive indices.

Not all of the above processes were fully modeled in my work. The purpose of this chapter is to summarize the way in which these processes were treated and to justify the reasons for neglecting to treat some of them.

I begin by describing the environment in which these processes take place, i.e., the model planet's atmosphere.

2.1 The model atmosphere

The background of this work and the environment where the grains are assumed to be is the radiative portion of the atmosphere of a giant planet, during the second phase of its evolution in the core accretion model. Specifically, I use model atmospheres kindly supplied by O. Hubickyj. The reasons for considering only the radiative zone of the atmosphere were twofold: First, it is the opacity in this zone that determines the rate of energy release from the planet into space and thus influences strongly the evolution time of the planet.

Second, being limited to the radiative zone allowed me to make some simplifying assumptions and to defer dealing with some of the physical processes that were harder to model.

In the following a reference to "the atmosphere" is always taken to mean the radiative part of the atmosphere.

Table 2.1 shows typical values of some properties of the atmosphere. The atmosphere and its properties are assumed to be a *static* background to the evolution of the grain population, even though the atmosphere itself is part of an evolving planet. It turns out that the time it takes the grain population to reach a steady state is indeed short compared with the evolution time scale of the planet (see Ch. 4). The atmosphere is also known to be quiescent (nonconvective).

2.2 Sedimentation

The sedimentation velocity of a solid grain is determined by equating the drag force that acts on it with the force of gravitation. In the case of a dilute gas

(large Knudsen number) the force of drag on a particle of radius a is given by

$$F = \frac{4\pi a^2 \rho_{\rm g} v_{\rm T} v_{\rm sed}}{3}. \tag{2.1}$$

In Eq. (2.1) $\rho_{\rm g}$ is the gas density, $v_{\rm T}$ is the thermal velocity of a gas molecule given by $\sqrt{8kT/\pi m}$ where k is Boltzmann's constant T the gas temperature and m is the mass of a gas molecule, and $v_{\rm sed}$ is the relative speed between the solid particle and the gas – the sedimentation speed. If the gas is non-dilute (Knudsen number smaller than one) then the drag force is given by

$$F = 6\pi a \eta v_{\rm sed}, \tag{2.2}$$

where η, the viscosity of the gas, is given by $\eta = 8.6 \times 10^{-7}\sqrt{T}$ kg m^{-1} s^{-1} (Podolak et al., 1988). Since we are dealing with grains ranging from microns to centimeters in size, in an atmosphere where the mean free path varies between 10^{-5} and 10^{-1} m, the Knudsen number Kn (ratio of the mean free path to particle size) will at times be much greater than, and much smaller than one, and at times close to one. A formula for the drag force that covers all cases is

$$F = \frac{6\pi a \eta v_{\rm sed}}{\psi}, \tag{2.3}$$

where ψ is an interpolating function that bridges the cases of small and large Knudsen number:

$$\psi = 1 + Kn\left[A + Be^{-C/Kn}\right] \tag{2.4}$$

with $A = 1.249$, $B = 0.42$, and $C = 0.87$ empirically derived constants (Kasten, 1968).

The sedimentation speed of a particle of size a and density ρ is then given by

$$v_{\rm sed} = \frac{2\pi a^2 \rho\, \psi g}{9\,\eta}. \tag{2.5}$$

Note that g and η are functions of the particle's height in the atmosphere. Typical velocities for a small grain, say $a = 1$ μm, range from 10^{-5} to 10^{-2} m/s, while a large grain, $a \approx 1$ cm, can reach speeds of tens of meters per second.

I include a small correction to the sedimentation velocity that is supposed to account in an approximate way for the flow of the background gas. Since there is a constant gas input being accreted at the top of the atmosphere I assume a downward gas flow everywhere in the atmosphere with a local velocity such that the flux at any point is equal to the flux of accreted gas. A grain's velocity relative to the height grid is then equal to its velocity relative to the gas, given by (2.5), plus the local velocity of the background gas flow which is equal to the gas accretion rate divided by the local gas density. This additional velocity term, the same for all grain sizes, is usually negligible for grains larger than ~ 500 μm but can be comparable to the velocity relative to the gas for very small grains. It is an approximation because, while significant quantities of gas may be added at the top of the atmosphere, the temperature density and pressure profiles are still assumed to be constant with height.

2.3 Collisions and coagulation

It is impossible, of course, to follow the trajectories of all particles in the atmosphere even with a powerful computer. Instead, statistical methods are used to estimate the number of collisions between grains.

Grains come into contact as a result of their relative velocities. One mechanism causing relative velocities between grains is their random (Brownian) motion. The expected number of collisions per second between two grains in a unit volume as a result of their random motions is (Fuchs, 1964, Ch. VII)

$$P_1(a_1, a_2) = 8\pi\langle a\rangle\langle D\rangle \left[\frac{\langle a\rangle}{\langle a\rangle + \langle\delta\rangle/2} + \frac{4\langle D\rangle}{\langle v_\mathrm{T}\rangle\langle a\rangle}\right]^{-1}. \tag{2.6}$$

In Eq. (2.6) $\langle a\rangle = \frac{1}{2}(a_1 + a_2)$ is the average grain radius and $\langle D\rangle = \frac{1}{2}(D_1 + D_2)$ is the average diffusion coefficient, where the coefficient for one particle is given by

$$D_i = \frac{3kT}{4\pi a_i^2 n_\mathrm{g} m_\mathrm{g} v_\mathrm{g}}, \tag{2.7}$$

n_g being the number density of the ambient gas, m_g the mass of a gas molecule, and v_g its thermal velocity. The average thermal velocity of two grains with velocities $v_{\mathrm{T}1}$ and $v_{\mathrm{T}2}$ is given by $\langle v_\mathrm{T}\rangle = (v_{\mathrm{T}1}^2 + v_{\mathrm{T}2}^2)^{1/2}$. The correction factor δ takes into account the fact that a grain much larger than a gas molecule does not change its course immediately after one collision with a molecule. If $l_\mathrm{B} = 8D/\pi v_\mathrm{T}$ is the distance traveled by a grain before its direction is significantly changed then

$$\delta = \frac{\sqrt{2}}{6a\, l_\mathrm{B}}\left[(2a + l_\mathrm{B})^3 - (4a^2 + l_\mathrm{B}^2)^{3/2}\right] - 2a, \tag{2.8}$$

and $\langle\delta\rangle = (\delta_1^2 + \delta_2^2)^{1/2}$.

If there are n_1 particles of size a_1 in a unit volume and n_2 particles of size a_2, and if the probability of collision between any pair is independent of all other collisions, than the number $N_1(a_1, a_2)$ of collisions per second between an a_1 particle and an a_2 particle is the probability $P_1(a_1, a_2)$ times the number of different pairs, or

$$N_1(a_1, a_2) = P_1(a_1, a_2) n_1 n_2. \tag{2.9}$$

The same is true for collisions between two particles of the same size except that the number of pairs is now $n_i^2/2$:[1]

$$N_1(a_1, a_1) = \frac{1}{2} P_1(a_1, a_1) n_1^2. \tag{2.10}$$

Another way for two grains to collide is when a larger grain overtakes a smaller one because of its faster sedimentation speed. The number of such collisions a single a_1 particle will experience in a second is

$$\pi(a_1 + a_2)^2 \left|v_\mathrm{sed}(a_1) - v_\mathrm{sed}(a_2)\right| n_2,$$

[1] Actually, the number of pairs is $n(n-1)/2$ but we assume there are many particles otherwise the collisions would not be independent.

and we may write

$$P_2(a_1, a_2) = 4\pi\langle a\rangle^2 \left| v_{\rm sed}(a_1) - v_{\rm sed}(a_2) \right|, \tag{2.11}$$

and

$$N_2(a_1, a_2) = P_2(a_1, a_2) n_1 n_2 \tag{2.12}$$

for the number of collisions due to overtaking in a unit volume in a unit time. Since $P_2(a_i, a_i) = 0$ we can have $P = P_1 + P_2$ and

$$N(a_i, a_j) = P(a_i, a_j) n_i n_j (1 - \frac{1}{2}\delta_{ij}) \tag{2.13}$$

for the total number of collisions.

The probability that grains will adhere after a collision, represented by a "sticking coefficient", is in reality dependent on the collision velocity, and probably on many other parameters. There is experimental evidence (Chokshi et al., 1993) that for small collision speeds and small grains the sticking coefficient is very close to one, and for most of the following I will assume that the grains stick on every collision, experimenting briefly with smaller (but still constant) sticking probability. The *coagulation kernel* is the combination of collision probability P and sticking probability γ:

$$K(a_i, a_j) = \gamma P(a_i, a_j). \tag{2.14}$$

2.4 Evaporation and condensation

The rate of mass loss due to evaporation is highly dependent on the composition of the grain and the ambient temperature. In the radiative zone the temperature is too low for any evaporation of rock, the assumed grain material in this work. For this reason evaporation is entirely neglected here. Evaporation would have to be accounted for in a model that follows the grains deeper into the atmosphere, or one that includes ice grains.

2.5 Opacity

In the outer portion of the protoplanet's atmosphere energy is transported mainly by radiation. The effectiveness of radiative transfer depends on the *opacity* of the atmosphere, a measure of the ability of photons to move freely in the gas, and on the temperature gradient in the atmosphere.

The opacity, or absorption coefficient, κ_ν, is defined by the amount of reduction in the intensity I of a beam of radiation of frequency ν, that passes through a length ds of matter with density ρ:

$$dI = -\kappa_\nu \rho I ds. \tag{2.15}$$

The value of the opacity, for a given frequency depends on the material of the scattering particle, through its refractive index, and also on its size. Here I use the following approximation to Mie scattering (van de Hulst, 1957; Cuzzi) to calculate the effective cross-section σ_ν of a grain of size a to scattering of radiation in the frequency ν.

The *size parameter*, $x = 2\pi a/\lambda$, divides the distribution into "small" grains ($x << 1$) and "large" grains ($x >> 1$), relative to the wavelength λ of incident radiation. In practice, a transition value of $x_0 = 1.3$ is used to separate the two regions. The scattering efficiency Q_s of the grain is approximated by

$$Q_s = \begin{cases} \frac{8x^4}{3}\frac{(n_r^2-1)^2}{(n_r^2+2)^2} & \text{for } x < 1.3, \\ 2x^2(n_r-1)^2(1+(\frac{n_i}{n_r-1})^2) & \text{for } x \geq 1.3, \end{cases} \tag{2.16}$$

where n_r and n_i are the real and imaginary refractive indices of the grain material respectively. The absorption efficiency Q_a is approximated, for all grain sizes, by

$$Q_a = \frac{24xn_rn_i}{(n_r^2+2)^2}. \tag{2.17}$$

The sum of the absorption and scattering efficiencies is corrected for the degree of overall forward or backward scattering to give the extinction efficiency,

$$Q_e = Q_a + Q_s(1-g), \tag{2.18}$$

where g, the asymmetry parameter, is approximated by

$$g = \begin{cases} 0.2 & \text{if } x < 2.5 \text{ and } n_i < 3, \\ 0.8 & \text{if } x > 2.5 \text{ and } n_i < 3, \\ -0.2 & \text{if } x < 2.5 \text{ and } n_i > 3, \\ 0.5 & \text{if } x > 2.5 \text{ and } n_i > 3, \end{cases} \tag{2.19}$$

and the effective cross-section is simply

$$\sigma_\nu = Q_e\pi a^2. \tag{2.20}$$

This approximation gives values for the scattering and absorption efficiencies that are usually within a factor of 1.5 of the values obtained with a full Mie theory calculation.

Knowing the number density of grains of this size, $n(a)$, their contribution to the opacity of the atmosphere is

$$\kappa_\nu(a) = \sigma_\nu(a)n(a)/\rho_{\text{gas}}, \tag{2.21}$$

assuming here that the density of the gas in the atmosphere is much higher than the density of solid grains, so that ρ in Eq. (2.15) can be taken as the gas density. The contribution from all grains is of course the sum, or integral, of the contribution from every grain size.

Models of the structure of planets, or stars, use an equation that directly relates energy flux with the temperature gradient and an "average" opacity:

$$H = \frac{4ac}{3\bar{\kappa}\rho}T^3\frac{dT}{dr}. \tag{2.22}$$

In Eq. (2.22) a is the radiation constant and c the speed of light. The connection between the specific opacity κ_ν and the mean opacity $\bar{\kappa}$ is given by (e.g., Clayton, 1968)

$$\frac{1}{\bar{\kappa}} = \frac{\int_0^\infty \frac{1}{\kappa_\nu}\frac{dB_\nu}{dT}\,d\nu}{\int_0^\infty \frac{dB_\nu}{dT}\,d\nu}, \tag{2.23}$$

where B_ν is Planck's source function

$$B_\nu(T) = \frac{2h\nu^3}{c^2}\frac{1}{\exp(h\nu/kT) - 1}, \tag{2.24}$$

h being Planck's constant. Equation (2.23) is known as the *Rosseland mean opacity*.

In the following chapter I describe the steps needed to model these physical processes in a computer program. Most are straightforward but some require explanation.

Chapter 3

Method

Using the definitions of Ch. 2 we can write an equation for the rate of change in number density of particles with mass m:

$$\frac{\partial n(m,r,t)}{\partial t} = \frac{1}{2}\int_0^m N(m', m-m', r, t)\, dm' - \int_0^\infty N(m, m', r, t)\, dm' - \boldsymbol{\nabla}\cdot\big(n(m,r,t)\mathbf{v}_{\rm sed}(m,r)\big) + Q(m,r,t). \quad (3.1)$$

In Eq. (3.1) the first integral on the right-hand-side gives the number of particles with mass m newly created by coagulation of particles with masses m' and $m-m'$, taking care not to double count the number of such collisions. The second integral on the rhs is the number of particles of mass m that grow to a larger mass by collision with some other particle. The divergence term gives the net number of particles that flow into or out of the region of the point r by sedimentation. We assume that the grains sediment only in the radial direction so that

$$\boldsymbol{\nabla}\cdot(n\mathbf{v}_{\rm sed}) = -\frac{\partial(nv_{\rm sed})}{\partial r} - \frac{2nv_{\rm sed}}{r}.$$

(Recall that $v_{\rm sed}$ was defined with a positive value in Eq. [2.5], which makes $\mathbf{v}_{\rm sed} = -v_{\rm sed}\hat{\mathbf{r}}$.)

The Q in Eq. (3.1) is a source term giving the number of particles that are injected into the atmosphere at the point r. Corresponding with the structure of the atmosphere at a given time I have information about the rate of accretion of gas and planetesimals from the core accretion models of Hubickyj et al., and these provide two sources for new grains. First, the nebular gas that is accreted onto the planet contains a certain amount of solid material, usually taken as 1% by mass. Second, planetesimals falling through the atmosphere break up and ablate and deposit solid grains during their flight. Hubickyj et al. calculate the profile of this mass deposition, i.e., the fraction of a planetesimal's mass that is injected in every height in the atmosphere. (In the core accretion model this is necessary for obtaining the amount of energy deposited in different levels of the atmosphere.) I usually assume that all this mass is in the form of grains with one size, although in reality there will be some distribution of sizes, different for different levels. The source term, like the structure of the atmosphere, is constant in time, for the interval being considered.

Equation (3.1), an integro-differential equation, cannot be solved analytically except in simple, unphysical cases. One way to treat such an equation is to approximate it with a set of algebraic equations, converting integrals to sums, and derivatives to differences, and proceed to solve numerically. I chose to take the different approach of a simulation, or physical modeling. That is, instead of translating and numerically solving an equation such as Eq. (3.1) I try to model directly the variables and physical processes in a computer program that tracks their evolution in time. These two approaches should be equivalent and a choice of one is partly a personal preference. For well known differential equations, like the wave equation or the equation of diffusion, there are highly specialized numerical algorithms with proven efficiencies and error estimates, so the first approach is clearly preferable. In the present case however, I felt that the physical system of interest, namely the size distribution of grains, has an inherently discrete nature. In a given population of particles that is controlled by coagulation (as opposed to evaporation for example) there is a discrete and finite number of particle sizes, and even a discrete and finite number of *possible* sizes, namely all integral multiples of the smallest particle, up to a particle mass that is the total mass of the system. It is because of the large number of particles and the "smallness" of the smallest particle that the system can be treated as continuous. Thus the first integral in Eq. (3.1), for example, is itself an approximation, to the more physical "sum over pairs".

In this chapter I describe the procedures I have used and some technical details. I also describe here some tests that were performed to confirm the validity of my code.

3.1 Modeling the atmosphere

The atmosphere files supplied by Hubickyj contain columns for gas density, temperature, and pressure, at given heights in the atmosphere. I regard these height grid points as the boundaries of a set of *layers* or *zones*. Thus, l grid points define $l-1$ layers. The properties of a layer, e.g. temperature, density, are averaged from the values of the corresponding property on the boundaries. Other properties such as viscosity, acceleration of gravity, etc. are derived based on these average values, and regarded as constant throughout the layer. A typical atmosphere has ~ 50 layers. (Recall that this is only the radiative zone of the planet's atmosphere.) The layers are numbered starting with the outermost, i.e., r_1 is the radius of the upper boundary of the top layer, r_2 is the radius of the boundary between this layer and the next one down, and so on.

3.2 Modeling the grains

I define a set of size *bins* to represent the size distribution of grains. All grains belonging to a bin are assumed to have the same size, a size distribution inside a bin was not considered (although it may be necessary in future work, see Sec. 4.7).

I assume that grains are made from monomers of a certain size a_0 and are spherical. In reality grains are likely to have a fractal structure (Weidenschilling and Cuzzi, 1993) that may effect their mechanical and optical properties. If

m_0 and ρ_0 denote the mass of the monomer and its density, respectively, then a grain composed of k monomers will have a mass of km_0 and a radius of $a_0 k^{1/3}$, and the same density ρ_0. Thus a suitable set of size bins would be

$$a_k = a_0 k^{1/3} \qquad k = 1, 2, \ldots. \tag{3.2}$$

Unfortunately, this would require an unreasonably large number of bins to cover the range of grain sizes. Instead, I use a sequence of size bins such that each grain has twice the mass of a grain in the previous size bin, or

$$a_k = a_0 2^{k/3}. \tag{3.3}$$

Spacing the size bins further apart is not recommended, a collision between two grains of the same size bin would not be enough to create one grain of the next size bin, and the efficiency of coagulation growth will be greatly (and artificially) reduced. Spacing the bins closer together, and allowing more bins to compensate, increases the computation time with little benefit. The number density of grains in the k-th size bin and j-th layer is denoted $n(j, k)$.

Allowing a finite number of bins means setting an artificial limit on grain size. There is a physical limit to grain size, a grain's mass cannot exceed the total mass of the system, but this limit requires an impractical number of bins. Computation time increases rapidly with the number of allowed bins while taking too few bins artificially stops the grain growth too soon. The following test proved useful in determining a suitable number of bins. I run the model without a source term and note the time it takes some fraction, say 90%, of the mass of solids to sediment out of the atmosphere, starting with a small number of size bins and increasing this number progressively. As more bins are used and the grains are allowed to reach larger sizes this "emptying time" generally becomes shorter, but ultimately steadies at a certain time that does not change when more bins are added. It is then plausible to assume that, even with an active source of small grains, adding more bins will not change the size distribution as grains will not have time enough to grow into the larger sizes. This would be true unless the source term is too large to be balanced by sedimentaion, a condition that can be checked easily.

3.3 Modeling sedimentation

The sedimentation velocity of each grain size in each layer can be computed once at the beginning of the program. Then, at some time t, the rate of change of grain number density for grains in size bin k and layer z is computed by taking the number of grains of this size that enter the layer through its upper boundary, and subtracting from it the number of grain that leave the layer through its lower boundary. The number of grains that pass through the upper boundary per second is

$$F_{\text{in}} = n(z-1, k) v_{\text{sed}}(r_{z-1}, a_k) \times 4\pi r_z^2,$$

and the number of grains per second passing through the lower boundary is

$$F_{\text{out}} = n(z, k) v_{\text{sed}}(r_z, a_k) \times 4\pi r_{z+1}^2.$$

Then the rate of change of the number density due to sedimentation is

$$\frac{\partial n(z,k)}{\partial t} = \frac{n(z-1,k)v_{\rm sed}(r_{z-1},a_k)\,4\pi r_z^2 - n(z,k)v_{\rm sed}(r_z,a_k)\,4\pi r_{z+1}^2}{\frac{4\pi}{3}(r_z^3 - r_{z+1}^3)}. \quad (3.4)$$

When grains leave the lowermost layer they are no longer tracked by the program, but a record is kept of the total mass that had sedimented out of the system.

3.4 Modeling coagulation

The coagulation kernel of Sec. 2.3 can be calculated once, for all bin sizes and layers, at the beginning of the program, and stored in a three dimensional array of `number of layers` × `number of bins` × `number of bins` elements. Then, at any time t, the number of collisions per second leading to coagulation in a unit volume in layer z, between a grain from size bin i and a grain from size bin j is

$$N(z,i,j) = K(z,i,j)n(z,i)n(z,j)(1 - \frac{1}{2}\,\delta_{ij}). \quad (3.5)$$

Now a grain of size i has a mass $m(i)$ and a grain of size j has a mass $m(j)$, and together they create one grain with a mass of $m(i)+m(j)$. In general there will not be a size bin whose corresponding mass is exactly this sum. Instead, the mass of the newly formed grain will fall somewhere between the masses of bins k and $k+1$, and the new grain should be counted as belonging to one of these bins or the other. Following Kovetz and Olund (1969) I define an array $C(i,j,k)$ giving the probability that, upon coagulation of a grain of size bin i with a grain of size bin j, a grain of the size bin k will be created:

$$C(i,j,k) = \begin{cases} \frac{m(i)+m(j)-m(k-1)}{m(k)-m(k-1)} & \text{if } m(k-1) < m(i)+m(j) \le m(k), \\ \frac{m(k+1)-m(i)-m(j)}{m(k+1)-m(k)} & \text{if } m(k) < m(i)+m(j) \le m(k+1), \\ 0 & \text{otherwise.} \end{cases} \quad (3.6)$$

This ensures that mass will be conserved, on the average, independent of the spacing between size bins.

The number of k-bin grains that are added, per second, to a unit volume in layer z is found by summing up all the different collisions that create a k-bin grain:

$$n(z,k)_+ = \sum_{\substack{1\le i\le k-1 \\ 1\le j\le i}} N(z,i,j)C(i,j,k). \quad (3.7)$$

Note that in Eq. (3.7) i goes up only to $k-1$. While it is possible for a collision between a k-bin grain and a much smaller grain to result in a k-bin grain, according to our scheme, this collision does not *add* a grain to the k-bin count, as one of the "constituents" was taken from this bin. The sum need not go higher than k because $C(i>k,j,k) = 0$.

The number of grains that should be subtracted from bin k is found by summing over all collisions between a k-bin grain and some other grain:

$$n(z,k)_- = \sum_{0\le i<\infty} N(z,k,i)(1 - C(k,i,k))(1+\delta_{ik}). \quad (3.8)$$

In Eq. (3.8) the summation goes up to whatever the number of bins was chosen to be, denoted by ∞. The term $(1 - C(k, i, k))$ is the probability that the collision will create a grain that belongs outside of the k bin. The $(1 + \delta_{ik})$ term is needed because when a k-bin grain collides with another grain of the same size, *two* grains are removed from the bin. Adding Eqs. (3.7) and (3.8) and substituting into Eq. (3.5) we get the expression for the rate of change in number density due to coagulation,

$$\frac{\partial n(z,k)}{\partial t} = \sum_{\substack{1\le i\le k-1\\ 1\le j\le i}} K(z,i,j)n(z,i)n(z,j)(1-\frac{1}{2}\,\delta_{ij})C(i,j,k) - n(z,k)\sum_{1\le i<\infty} K(z,k,i)n(z,i)(1-C(k,i,k)). \quad (3.9)$$

There remains still the question of what to do with those grains that grow beyond the largest bin. As many bins as are allowed in the distribution they will all contain, after enough time has passed, at least a small fraction of the mass of grains. When grains of the largest bin collide with other grains, or between themselves, there is a chance according to our scheme that a grain will be formed that belongs in a larger bin. Discarding these grains from the distribution, or keeping them in their original bin, means that over time mass will be lost from the system. This is not a very serious problem in terms of the resulting distribution because the number of bins was chosen in a way that ensures that most of the grains will be accomodated. But there is a simple way to correct this problem and ensure conservation of mass. After determining the desired number of bins for the distribution, say N_B, one or two extra bins are added and used to "recycle" mass back into the distribution: After every time step the small amount of mass that accumulated in bins $N_B + 1$ and larger is returned to bin N_B and the number density of the larger bins is reset to zero. If the bin spacing (3.3) is used than one extra bin is enough to ensure mass conservation but more bins are needed when a finer distribution is used.

It may be worth noting here that the calculation of Eq. (3.9), involving a triple sum over size bins, is the main time consuming routine in the program. There may be ways to optimize this routine to reduce the computational load but I have not explored this.

Once the rate of change due to the combined effects of coagulation, sedimentation, and the source term is calculated, a time step is chosen, small enough to ensure that the total change in number density at the end of the time step for every size bin and in every layer will not exceed one per cent of the number density at the beginning of the time step.

3.5 Comparison with analytical solutions

As a check on the coagulation algorithm described above I have used it to model some special cases that can also be solved analytically, running the program with sedimentation disabled and focusing on one layer. The analytic solutions require that all possible grain masses have corresponding size bins, i.e., that the size bins be spaced according to Eq. (3.2). The coagulation equation may

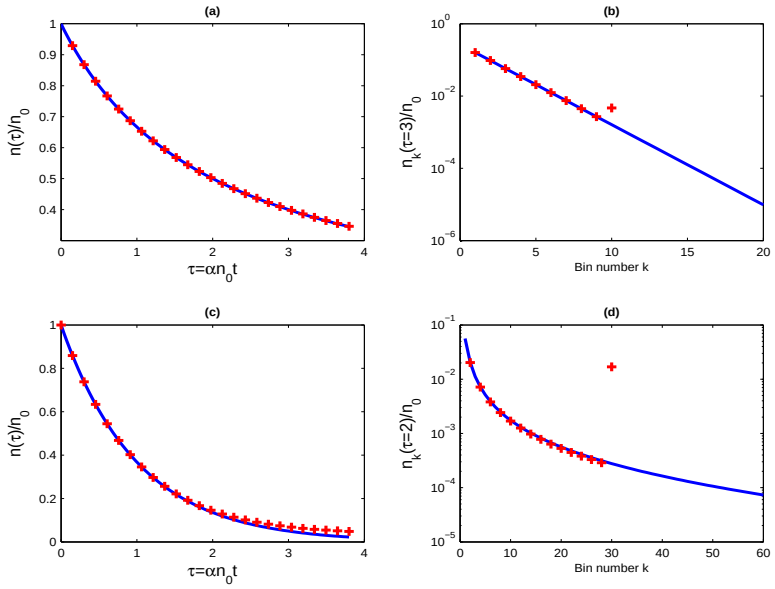

Figure 3.1: Analytic solutions to the coagulation equation (3.10). In the case of a constant kernel, (a) Fraction of particles left after time τ, in dimensionless time units. (b) Distribution of particles in size bins. And in the case of a linear kernel, (c) Fraction of particles after time τ, and (d) Distribution in size bins. The solid lines all show the shape of the analytical function and the plus markers show the corresponding values from numerical calculation.

then be written in the more compact form,

$$\frac{d}{dt}n(k) = \frac{1}{2}\sum_{i+j=k} K(i,j)n(i)n(j) - n(k)\sum_{i=1}^{\infty} K(i,k)n(i). \tag{3.10}$$

The simplest case is the constant kernel, $K(i,j) = \alpha$. With all grains initially in the smallest size bin, the total number of grains in the distribution that are left after t seconds is found to be (Wetherill, 1990)

$$n(t) = n_0(1 + \frac{1}{2}\alpha n_0 t)^{-1} = n_0 f(t), \tag{3.11}$$

where n_0 is the number of grains at $t = 0$. The complete solution, the number of grains in bin k for $t > 0$, is

$$n_k(t) = n_0 f(t)^2(1 - f(t))^{(k-1)}. \tag{3.12}$$

These solutions are shown in Fig. 3.1 along with the results of the numerical simulation. The numerical results agree exactly with the analytic solution. The extra grains in the last bin in the simulation (Figs. 3.1b and d) are the result of *having* a last bin, that grains can grow into but not out of. The number of grains in the last bin should be interpreted as representing all the grains of that size *and larger*, or as the total number of grains in the tail of the analytic distribution.

Another case that can be solved analytically is that of a linear kernel, $K(i, j) = \beta(i + j)$ (Wetherill, 1990). The number of grains that remain after time t in this case is

$$n(t) = n_0 \exp(-\beta n_0 t) = n_0 f(t), \tag{3.13}$$

and the distribution is

$$n_k(t) = n_0 \frac{k^{(k-1)}}{k!} f(t)(1 - f(t))^{(k-1)} \exp\big(-k(1 - f(t))\big). \tag{3.14}$$

These functions are also compared with the results of simulation in Fig. 3.1. Again, the numerical results agree well with the analytic solution until enough time has passed that a significant number of grains is in the tail of the distribution, above the largest bin used in the simulation.

While these tests are not applicable in the case of a real, physical kernel, they provide some measure of confidence in the numerical algorithm. In the next chapter I discuss the results of running the model with realistic parameters, the opacities that result from these runs, and their implications for models of planet formation.

Chapter 4

Results

In this chapter I present the results of grain opacity calculations, made using the procedures described in chapter 3 and under the assumptions described in chapter 2. Within the bounds of these assumptions there are still some parameters left uncertain, the most important of these is perhaps the assumed size of the monomers. Other parameters, like the grain material (manifested in its density and refractive index), the sticking coefficient, or the exact ratio of dust in the nebular gas, can also be experimented with to some degree. While I have not mapped out the parameter space methodically, I have experimented sufficiently with various scenarios to arrive, I believe, at a consistent picture. This picture is presented here in the form of "perturbations" about a baseline scenario. I then discuss the conclusions that can be drawn from these results.

4.1 Baseline scenario

A set of nominal values for the model parameters forms a baseline for comparison. The full set of parameters is given in Table 4.1. The monomer size is 1 μm, the sticking coefficient is 1.

With this configuration I ran the program on three atmosphere files representing the structure of the protoplanet's atmosphere at roughly the beginning, the middle, and the end of phase 2 (see Ch. 1). The distribution of grain sizes reaches a steady state after less than 1500 years[1], a small fraction of the time spent in phase 2, suggesting that the initial conditions, i.e., the initial distribution of grains throughout the atmosphere, is unimportant. The assumed initial distribution was that the atmosphere contains an amount of solids equal to one per cent of the gas mass in any given layer, and that these grains are all in the form of monomers.

Figure 4.1 shows the steady state size distribution of grains in several layers of the atmosphere, at 0.8 Myr, or roughly the middle of phase 2. Recall that small grains are continuously being deposited in all layers so we can expect a large population of small grains everywhere. As we move deeper into the atmosphere we find more and more large grains. These are grains that had time

[1]The condition for automatic determination of steady state was that the net rate of mass accretion into the atmosphere was zero, or that mass was leaving the atmosphere as fast as it was coming in. In principle there may be more than one size distribution that satisfies this condition. However in practice it was found that changes in the size distribution became undetectable before this steady state condition was met.

Table 4.1: Nominal values for model parameters.

Parameter	Value
Atmospheric gas properties	
Molecular weight (g/mol)	2.3
Collision cross-section (cm^2)	1.0×10^{-15}
Dust-to-gas ratio	0.01
Grain properties	
Matter density (g/cm^3)	2.8
Monomer size (m)	1.0×10^{-6}
Sticking coefficient	1.0
Other	
Size of planetesimals (km)	100.0
Size of accreted grains	same as monomer
Refractive index table	of Tholin

to grow while settling from higher up. In the lower layers a significant fraction of the total mass of solid grains is in the form of grains as large as 0.1 cm. An easier way to see the changes in the steady state size distribution throughout the atmosphere would be to look at some integrals of the distribution, plotted as a function of radius, as in Fig. 4.2. Figure 4.2 shows the averages of the two quantities that determine the opacity in each layer: the amount of solid matter present as grains, and the efficiency of these grains as scatterers, shown here by the average cross-section. Note however that to correctly determine the opacity we need to know the actual shape of the distribution and not just the averages. The mean geometric cross-section, for example, is nearly identical very high and very low in the atmosphere, but the distributions (Fig. 4.1) are very different. Figure 4.2 also shows how the grains' efficiency as scatterers, the extinction cross-section, can be very different from their simple geometric cross-section. As the temperature rises, the wavelength of the peak in the Planck spectrum decreases, and similar size distributions can have quite different opacities.

The grain opacity and optical depth throughout the atmosphere's radiative zone are shown in Fig. 4.3, for the starting distribution and for the steady state distribution. We see that while the opacity is quite high at first, it drops quickly when grains are allowed to grow, and the steady state opacity throughout most of the atmosphere is very much lower than 1 cm^2/g, the order of magnitude of interstellar opacity at these temperatures. Only the lower third of the atmosphere (but $\sim$90% of the mass) is consistent with the low opacity models[2] of Hubickyj et al., but the optical depth of the radiative zone is slightly lower than it would be with their low opacity.

Figures 4.4 and 4.5 show the opacities at roughly the beginning, 0.35 Myr, and the end, 1.3 Myr, of phase 2 respectively. The atmosphere and core of the protoplanet grow more massive with time, but the structure of the atmosphere, the (z, T, ρ) relation, is not radically different. The corresponding opacities show the same behavior that was observed in Fig. 4.3 – the steady state opacity is highest at the top of the atmosphere, where it is similar to the interstellar opacity, and decreases gradually bringing the lower third of the atmosphere to less than two per cent of the interstellar value.

The small *increase* in opacity in the very last few layers of the atmosphere

[2]Hubickyj et al. refer to the interstellar value of grain opacity as *high opacity*, and to 2% of this value as *low opacity*.

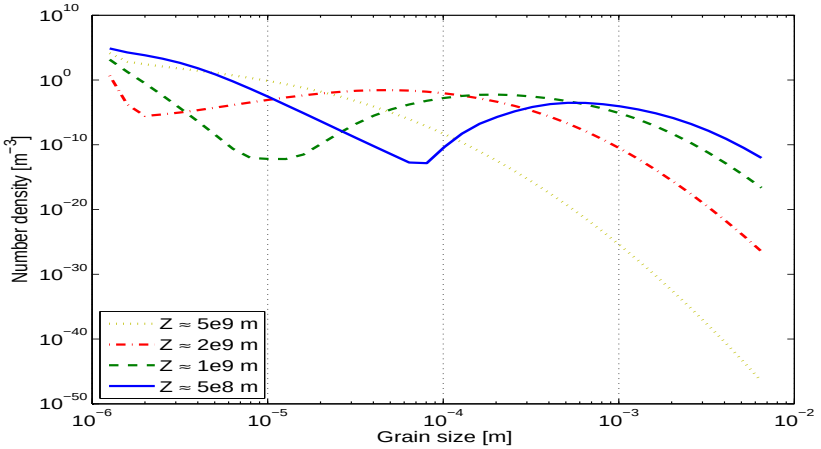

Figure 4.1: Steady state size distribution of grains. The atmosphere structure corresponds to the middle of phase 2.

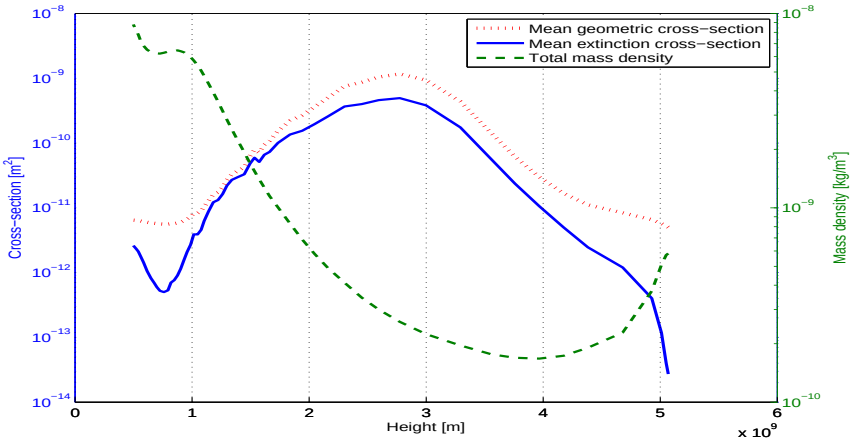

Figure 4.2: Integrals of the steady state size distribution. The extinction cross-section was calculated for the wavelength of maximum radiation at the layer's temperature.

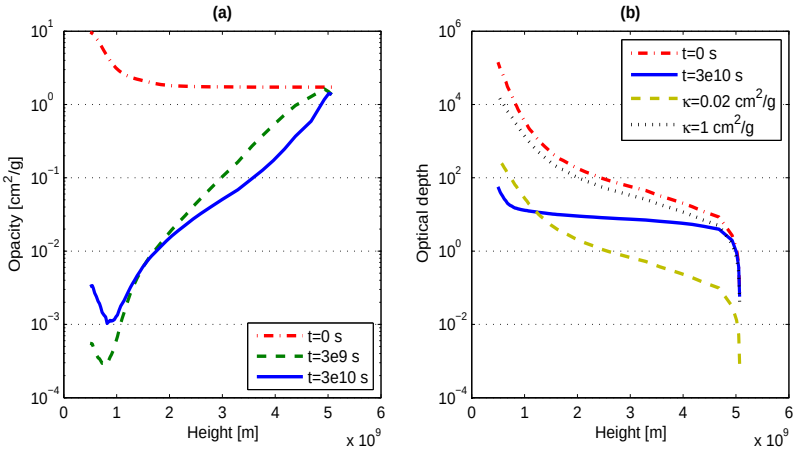

Figure 4.3: Grain contribution to opacity (a) and optical depth (b) of the starting and steady state distributions. Also shown in (a) is the opacity a short time after settling begins, and in (b) the optical depth profiles that result from taking a constant *High*, 1 cm^2/g, and *Low*, 0.02 cm^2/g opacities.

is puzzling at first. We see a similar feature in Fig. 4.2, with the increase of the mean extinction cross-section at approximately the same height. A clue for understanding this feature can be gained by looking at the behavior of the sedimentation velocity of larger grains, Fig. 4.6. In the upper atmosphere the drag force on all grains is described by the formula for a large Knudsen number (Eq. [2.1]) and is proportional to the gas density. The gas density is rapidly increasing as the grains move deeper into the atmosphere, increasing the drag force and slowing the sedimentaion. A short distance above the bottom of the radiative zone the gas density is high enough so that the *largest* grains enter the regime of a low Knudsen number, the drag force being proportional to the more slowly changing viscosity (Eq. [2.2]). With the drag force being almost constant, the increasing pull of gravity causes an increase in sedimentation velocity of larger grains, but not of smaller ones. This effect creates a small shift in the size distribution, increasing somewhat the opacity.

I focus next on one atmosphere structure, that of 0.9 Myr, with variations in the important model parameters.

4.2 Monomer size

Figure 4.7 shows the steady state opacity profiles calculated with four different monomers sizes. In every case the input grains, both from planetesimals and from nebular gas, are assumed to be composed of monomers only. It is interesting that while it takes somewhat longer for the distribution to reach a steady state when the monomers are larger, the size of the largest grains in the steady state distribution does not seem to depend on the monomer size.

The monomer size is obviously an important parameter. This is mostly due to the assumption that the constant influx of gas and planetesimals contains grain monomers. This constant flux sets a kind of “boundary condition” on the

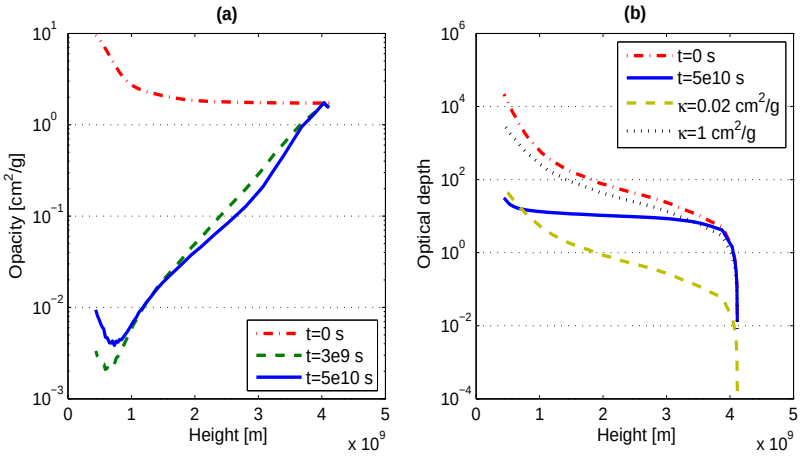

Figure 4.4: Same as Fig. 4.3 for a protoplanetary atmosphere at the beginning of phase 2 of core accretion.

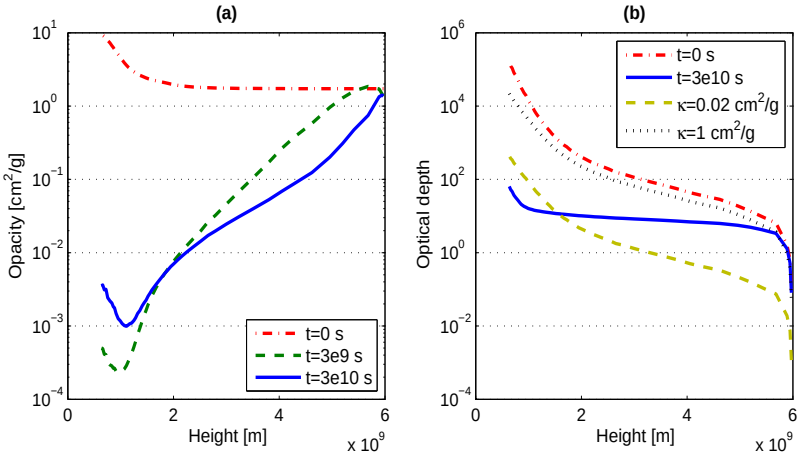

Figure 4.5: Same as Figs. 4.4 and 4.3 for a protoplanetary atmosphere at the end of phase 2.

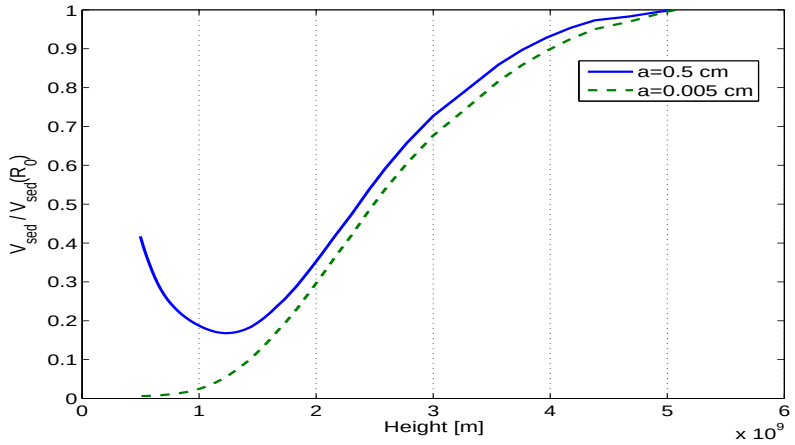

Figure 4.6: Trends of the sedimentation velocity of grains, comparing small grains with large ones.

steady state distribution that determines the concentration of monomer grains in every layer. The concentration of monomer grains determines, in turn, the rate of growth and thus the shape of the entire distribution. Surprisingly, the different opacity profiles seem to almost converge in the lower layers of the atmosphere, and in all cases the opacity is lower than interstellar, and the lower third of the atmosphere is consistent with the low opacity assumption of Hubickyj et al..

The fact that the opacity profiles are sensitive to the choice of monomer size is perhaps a drawback of the procedure used to calculate them. In particular there is no reason that the source of new grains will contain only monomers, or even contain monomers at all, but without processes that *reduce* the grain size, like breakup or evaporation, there is no reason to consider any grains smaller than those brought in from outside the planet. A more complete calculation would probably distinguish between *monomer size* – a somewhat arbitrary model parameter similar in nature to grid resolution or time step, and *source size* – a physical parameter determined from observation or independent calculations. In that case it can be hoped that the resulting opacity will be insensitive at least to the model parameter.

4.3 Sticking coefficient

As was mentioned before the fate of grains that undergo a collision, whether they stick together, or come apart with the same, or different masses, is a complicated question. For small grains and low collision velocities it is believed that coagulation is the most probable outcome (Chokshi et al., 1993). I tested the effect of using a sticking coefficient smaller than one to arbitrarily reduce the efficiency of coagulation. It turns out that the resulting opacity is mildly sensitive to changes in a constant sticking coefficient. The opacity profiles in Fig. 4.8 show the same behavior, with approximately the same values, for a range of sticking coefficients from 1 to 0.4. This may not be the case if a

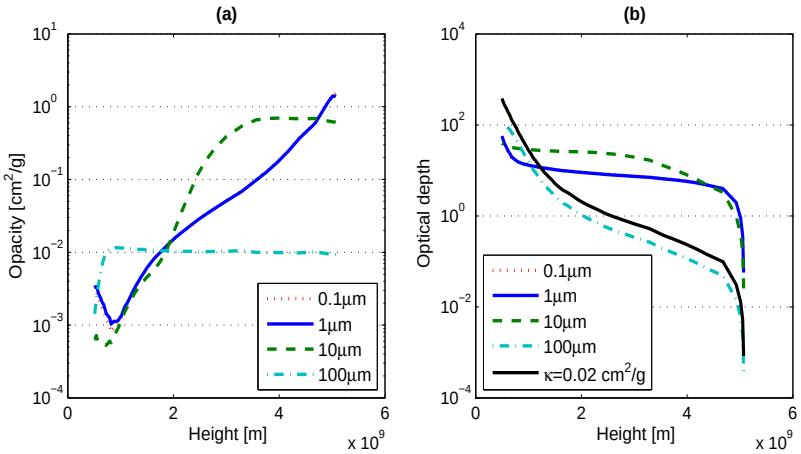

Figure 4.7: Effect of monomer size on the steady state opacity. (The curve for the case of 0.1 μm lies under the curve for 1 μm.)

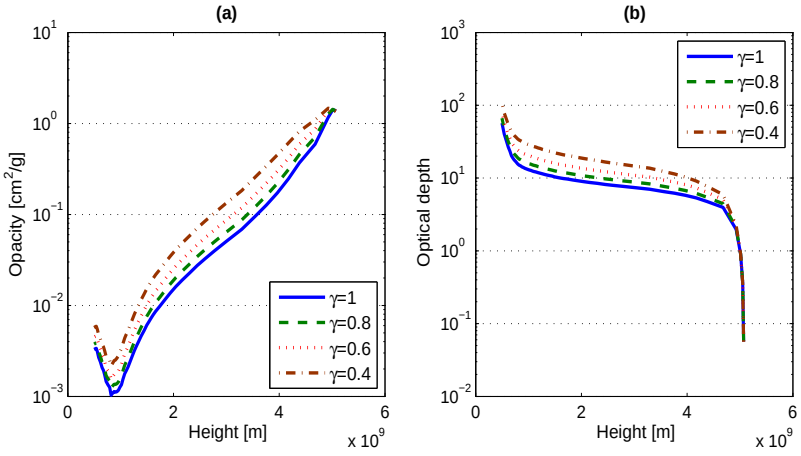

Figure 4.8: Effect of changing sticking coefficient on steady state opacity.

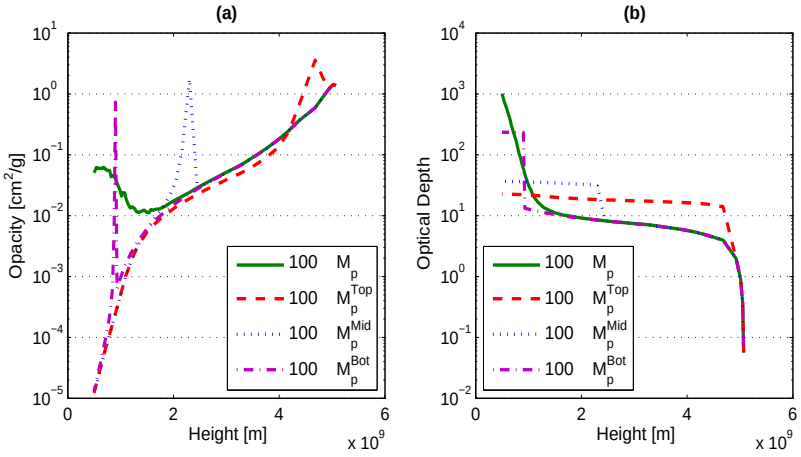

Figure 4.9: Increased input from planetesimals, accounting approximately to the possibility of smaller planetesimals. The line marked $100 \times M_p$ corresponds to increasing the planetesimal dust source by a factor of hundred, throughout the radiative zone, maintaining the mass deposition profile. The other lines correspond to placing the increased source of grains all in one layer, at approximately the top, the bottom, and the middle of the radiative zone.

"sticking function" will be used that differentiates small and large grains, and low and high collision speeds.

The time to reach a steady state increases somewhat when the sticking coefficient is lowered, but remains in the range of a few thousand years, much lower than the time scale of planet formation.

4.4 Planetesimal size

During most of phase 2 of core accretion the protoplanet gains on the order of 10^{-6} $M_\oplus$/yr of high-Z material from accreting planetesimals. But most of this mass is added to the planet's atmosphere *below* the radiative zone, or possibly added directly to the core. In their model of planet formation, Hubickyj et al. calculate first the rate of solid planetesimal accretion by the protoplanet, then calculate the interaction between a single planetesimal and the planet's atmosphere to determine how much mass and energy are deposited at different heights. They assume for the purpose of this calculation that the planetesimals all have a radius of 100 km. In general, smaller planetesimals are expected to deposit more of their mass higher up in the atmosphere while larger planetesimals deposit their mass deeper in the atmosphere or even survive to reach the core nearly intact.

Rather than repeat lengthy calculations with planetesimals of different sizes, I tested the effect of varying the assumed planetesimal size by varying directly the mass deposition profiles. In particular, I have tested some extreme cases such as adding all the mass that is deposited in the radiative zone only to the top layer, or some other layer, and increasing that amount until the *total* mass from accreting planetesimals is added to the radiative zone. Some of these cases are shown in Fig. 4.9.

Clearly, a change in the mass deposition profile from ablating planetesimals

can cause a significant change in the opacity profile, raising the opacity at some levels and lowering it elsewhere. For example, putting all the mass that accreting planetesimals bring into the planet in the upper atmosphere, in the form of small grains, causes a significant increase in the opacity of the highest layers and a much sharper decrease in the lower layers. This is probably because the very high concentration of small grains, those from ablating planetesimals in addition to those carried by infalling gas, increases the efficiency of the growth process, resulting in fewer of the small grains reaching the lower layers.

4.5 Other parameters

In the baseline scenario the grain opacity is calculated using a table of wavelength dependent refractive indices measured for tholins (Khare et al., 1984). Figure 4.10 compares this opacity profile with one calculated with a refractive index table measured for olivine (Dorschner et al., 1995).

The amount of solid matter that is contained in the nebular gas that is accreted by the planet should be close to one per cent of the gas mass. Figure 4.11 compares the opacity profiles obtained when this ratio is varied. It is interesting that when the amount of dust in the accreted gas is greatly reduced the opacity in the mid layers becomes significantly higher. This is again related to the efficiency of the growth process, which is dependent in a nontrivial way on the constant concentration of small grains dictated by the source term.

4.6 Conclusions

Before any conclusions can be drawn from the above results about the effect of grain growth on planet formation it is important to note again one important assumption of the calculations made here, the assumption of a static atmosphere. As was previously mentioned, the radius-density-temperature relation of the atmosphere remains constant throughout the calculation. This assumption was justified because the time to reach a steady state of the grain size distribution is much shorter than the time scale of the atmosphere's evolution. We must remember however that the structure of the atmosphere which is used in the present calculation was determined *without* knowledge of the grain size distribution, and with a prescribed grain opacity. The grain opacity itself can influence the evolution of the planet's atmosphere – this is just why we are interested in it. In this sense, the calculations carried out here are not completely self consistent: It is possible that using the opacity profiles shown above in a planet evolution model would result in different atmosphere structures which, if used as background for the grain growth process, would result in different opacity profiles.

With this reservation in mind, there is at least one conclusion that can still be stated with some confidence about the effects of grain growth on the atmosphere's opacity, and it is that grain growth *does affect* the atmosphere's opacity. More precisely: The conditions during phase 2 of core accretion are such that growth and settling are efficient processes by which grains are removed from the radiative zone of the planet's atmosphere, reducing their contribution to the opacity. For most of the radiative zone the resulting grain opacity is significantly lower than it would be if grain growth were not accounted for. The

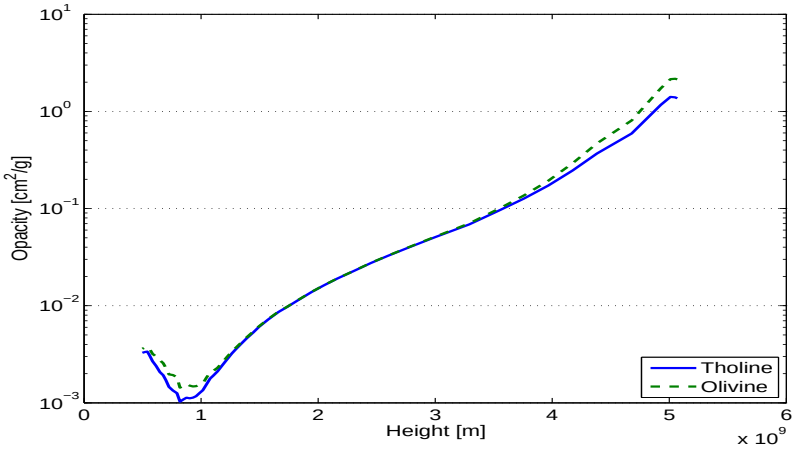

Figure 4.10: Comparison of the opacities of grains with refractive index of tholin and of olivine.

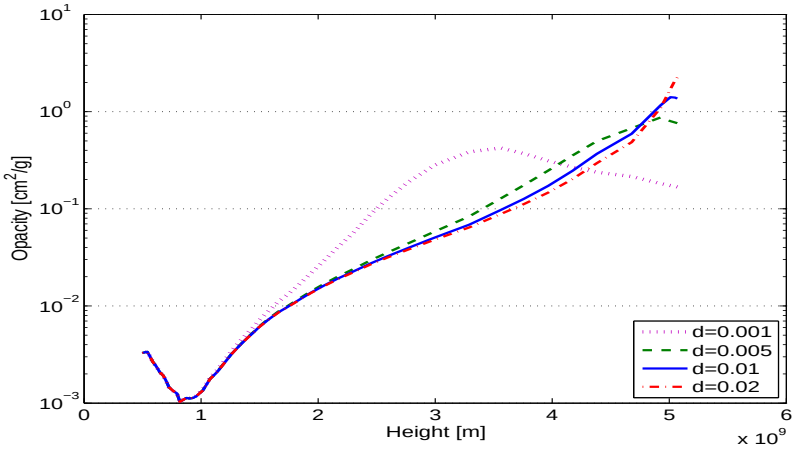

Figure 4.11: Comparison of opacity profiles obtained with several ratios of solid matter in nebular gas.

implication for giant planet formation theory would be that the formation time of a Jupiter-like planet through the core accretion scenario may be shortened, alleviating one of the major points of concern about this model.

As for the actual value of grain opacity that should be used in planet evolution models, I would suggest one of two options: The preferred option is to incorporate a grain growth and settling calculation, at least in an approximate way, into the evolution model. This will ensure a consistent treatment of the relationship between the atmosphere's structure and it's opacity. However this option also requires some work, modifying existing code, and it will, almost certainly, increase the computation time of evolution models.

If incorporating grain microphysics in a planet evolution code turns out to be impractical, it may still be possible to use grain opacity profiles created by an independent code with a representative atmosphere structure. The evolution code would presumably be halted at several points along the way and the atmosphere structure would be used to determine a steady state grain opacity profile. This opacity will then be taken as constant for the next period of evolution. This procedure will only work provided the grains reach a steady state in a short enough time.

4.7 Future work

As was discussed in chapter 2, the calculations of the grain size distribution carried out in the present work had involved some simplifying assumptions and had neglected some possibly important processes. In particular, three things that are likely to affect grain growth and size distribution are evaporation and condensation, breakup of grains due to collisions, and the fractal nature of grains. While I believe that the results presented in this chapter are still valid for the scenarios considered here, it would be desirable in future work to include these processes in the calculation and test their effect. This is particularly important if the grain growth calculation is to be incorporated into a planetary evolution model, as was suggested in the previous section.

In the present work, evaporation of grains was completely neglected. This was justified because at the temperature range that the grains were expected to experience there would be almost no evaporation of rocky material. If however we wish to continue tracking the grains into deeper layers of an evolving planet, the temperatures will eventually reach the melting point of rock. Also, if we would like to study icy grains then evaporation becomes significant even at the lower temperatures encountered at the top of the atmosphere. (A fraction of the high-Z mass that is accreted by the planet is certainly in the from of water ice. Assuming that all the accreted mass is refractory material leads perhaps to an upper limit estimate of the resulting opacity – if some of the material is ice, it will evaporate and lower the opacity. But this conclusion may not hold under all circumstances. Recall that reducing the amount of accreted matter eventually led to an *increase* in the mid layers' opacities [Fig. 4.11], as a result of the reduced efficiency of the coagulation process. It will be interesting to test the effect of including a reasonable amount of ice in the accreted mass.)

Including evaporation in the calculation of the growth rate of grains requires some modification of the size bin concept. The problem is that while coagulation through collision is a process that creates a discrete set of grain sizes,

evaporation reduces a grain's size smoothly, striping it molecule by molecule. With the size bin system, evaporation would progress in an uneven manner, either causing no change at all to the distribution, or emptying entire bins in a single time step. This can possibly lead to stability problems in the calculation, and is also a poor approximation of reality.

One modification that can be explored to overcome this problem would be to assume some size distribution of grains *inside* a size bin. For example, grains belonging to the size bin k could be thought of as distributed normally with a mean radius a_k, and a probability density that drops sharply when approaching the adjacent bins. In this way, losing an amount Δm of mass through evaporation in a time interval Δt, corresponds to some probability p that a grain would move from the size bin k to the bin $k-1$. This method would be appropriate only if the growth rate turns out to be insensitive to the exact choice of intra-bin distribution, or if an appropriate distribution can be chosen based on physical considerations.

Another assumption that was made in the present work was that grains stick after every collision. This assumption was justified because there exists experimental data that indicates that, at the typical collision velocity and grain size considered here, the grains are expected to stick with a probability close to one (Chokshi et al., 1993). It was also shown earlier (Fig. 4.8) that reducing the sticking probability arbitrarily, slows somewhat the growth rate but does not change very much the final size distribution. However under different conditions, such as may be encountered deeper in a planetary atmosphere,[3] a collision between grains need not result in coagulation, and may even result in breakup of one or both of the grains. This can change the size distribution of grains in steady state, as well as slow down the growth process considerably.

Including the possibility of breakup in the growth rate calculation would not be technically difficult. The sticking coefficient should be replaced with a "sticking function" that depends on grain size and velocity, and possibly composition. The value of this function will presumably be deduced from experimental data.

Finally, in the present work all grains were assumed to be spherical. Laboratory experiments (Bar-Nun et al., 1988) as well as numerical simulations (Weidenschilling and Cuzzi, 1993) indicate that the larger grains at least are expected to have a fractal nature. The fractal nature of the grains affects both their mobility in the gas, and thus their collision and growth rate, and their optical properties. It is possible to approximate the mobility of fractal grains with equivalent spherical grains with a density that is dependent on radius (Podolak, 2003); and to approximate the scattering efficiency of fractal grains with equivalent spherical grains that are porous and partially filled with a scattering material that has a complex refractive index of 1.0 (Podolak, 2003). Another possibility is to use empirical data to determine the mobility and optical properties of fractal grains.

[3]The collision velocity of small grains may become much higher if they are carried by the convective currents that exist in the deeper layers of the atmosphere.

Bibliography

A. Bar-Nun, I. Kleinfeld, and E. Ganor. Shape and optical properties of aerosols formed by photolysis of acetylene, ethylene, and hydrogen cyanide. *Journal of Geophysical Research*, 93:8383–8387, 1988. [cited on p. 30]

A. Chokshi, A. G. G. M. Tielens, and D. Hollenbach. Dust coagulation. *Astrophysical Journal*, 407:806–819, 1993. [cited on p. 5, 9, 24, 30]

D. D. Clayton. *Principles of stelar evolution and nucleosynthesis*. McGraw-Hill, 1968. [cited on p. 10]

J. Cuzzi. Personal communication. NASA Ames research center. [cited on p. 9]

J. Dorschner, B. Begemann, T. Henning, C. Jaeger, and H. Mutschke. Steps toward interstellar silicate mineralogy. ii. study of mg-fe-silicate glasses of variable composition. *Astronomy and Astrophysics*, 300:503, 1995. (Table 5). [cited on p. 27]

N. A. Fuchs. *The mechanics of aerosols*. Pergamon Press, 1964. [cited on p. 8]

K. E. Haisch, Jr., E. A. Lada, and C. J. Lada. Disk frequencies and lifetimes in young clusters. *Astrophysical Journal*, 553:L153–L156, 2001. [cited on p. 2]

O. Hubickyj, P. Bodenheimer, and J. J. Lissauer. Accretion of the gaseous envelope of jupiter around a 5–10 earth-mass core. *Icarus*, 179:415–431, 2005. [cited on p. i, 1, 2, 3, 4, 12, 20, 24, 26]

F. Kasten. Falling speed of aerosol particles. *Journal of applied meteorology*, 7:944–946, 1968. [cited on p. 7]

B. N. Khare, C. Sagan, E. T. Arakawa, F. Suites, T. A. Callcott, and M. W. Williams. Optical constants of organic tholins produced in a simulated titanian atmosphere - from soft x-ray to microwave frequencies. *Icarus*, 60: 127–137, 1984. [cited on p. 27]

A. Kovetz and B. Olund. The effect of coalescence and condensation on rain formation in a cloud of finite vertical extent. *Journal of the Atmospheric Sciences*, 26(5):1060–1065, 1969. [cited on p. 15]

M. Podolak. The contribution of small grains to the opacity of protoplanetary atmospheres. *Icarus*, 165:428–437, 2003. [cited on p. 3, 30]

M. Podolak, J. B. Pollack, and R. T. Reynolds. Interactions of planetesimals with protoplanetary atmospheres. *Icarus*, 73:163–179, 1988. [cited on p. 7]

J. B. Pollack, O. Hubickyj, P. Bodenheimer, J. J. Lissauer, M. Podolak, and Y. Greenzweig. Formation of the giant planets by concurrent accretion of solids and gas. *Icarus*, 124:62–85, 1996. [cited on p. 1, 3]

D. Saumon and T. Guillot. Shock compression of deuterium and the interiors of jupiter and saturn. *The Astrophysical Journal*, 609:1170–1180, 2004. [cited on p. 1]

A. G. G. M. Tielens, C. F. McKee, C. G. Seab, and D. J. Hollenbach. The physics of grain-grain collisions and gas-grain sputtering in interstellar shocks. *The Astrophysical Journal*, 431:321–340, 1994. [cited on p. 5]

H. C. van de Hulst. *Light scattering by small particles*. New York: John Wiley Sons, 1957. [cited on p. 9]

S. J. Weidenschilling and J. N. Cuzzi. Formation of planetesimals in the solar nebula. In E. H. Levy and J. I. Lunine, editors, *Protostars and Planets III*, pages 1031–1060, 1993. [cited on p. 13, 30]

G. W. Wetherill. Comparison of analytical and physical modeling of planetesimal accumulation. *Icarus*, 88:336–354, 1990. [cited on p. 17, 18]

List of Figures

List of Tables